PREPARATION AND CHARACTERIZATION OF COPPER MATRIX REINFORCED WITH COPPER-COATED SILICON CARBIDE COMPOSITES FOR ELECTRONIC PACKAGING

AZIDA BINTI AZMI

FACULTY OF ENGINEERING
UNIVERSITY OF MALAYA
KUALA LUMPUR

2012

PREPARATION AND CHARACTERIZATION OF COPPER/COPPER-COATED SILICON CARBIDE COMPOSITES FOR ELECTRONIC PACKAGING

AZIDA BINTI AZMI

RESEARCH REPORT SUBMITTED IN PARTIAL FULFILLMENT OF THE REQUIREMENT FOR THE DEGREE OF MASTER OF ENGINEERING

FACULTY OF ENGINEERING
UNIVERSITY OF MALAYA
KUALA LUMPUR

2012

ABSTRACT

Metal matrix composites (MMCs) have great potentials as packaging materials among other composite groups because the properties can be engineered to the design needs. Copper matrix reinforced with silicon carbide particles has greater potential due to the fact that it has higher thermal conductivity compared to the widely used aluminum. However, the bonding between the copper matrix and the SiC reinforcement must be improved since there is interface issues which affect the thermophysical properties of the CuSiC composites. Therefore, the SiC is coated with a thin copper film via electroless coating technique which is least expensive, simple and can provide homogenous copper deposits. The SiC is first need to be cleaned, etched, sensitized and activated to prepare the SiC particles surface for copper to be deposited onto it. Then, an electroless copper coating bath is prepared and the SiC is coated under suitable temperature and pH to obtain a good coating on SiC particles. Then, the CuSiC composites are fabricated via powder metallurgy methodology by ball milling to mix the copper matrix and SiC reinforcement. Then the mixture is pressed under uniaxial compaction loading and sintered at 925°C for 2 hours. Then the samples are ready for characterization and testing.

The SEM images showed the difference between the raw SiC and cleaned SiC after ultrasonically cleaned in solvent. After sensitizing and activation process, the SEM image showed that it has the catalytic elements during the activation process. Then, the SEM image after coating process showed the copper deposits on the SiC particles surface. The particle size distribution has increased from 45.639μm before cleaning to 45.993μm after cleaning. Then the size increased to 46.750μm after sensitizing and activation process. Then, the size increased to 48.100μm after coating process.

The CuSiC composite is lighter compared to the pure metal. Density for copper is 8.93g/cm^3. The density of CuSiC composites with Cu-coated SiC particles reinforcement is range from 7.48g/cm^3 to 3.44g/cm^3 with the volume fraction of the reinforcement varies from 0.1, 0.2, 0.3, 0.4, 0.5, 0.6 and 0.7. The percentage of porosity is increased with the increment of reinforcement volume fraction due to entrapped H_2 during coating process of the SiC particles reinforcement.

ABSTRAK

Komposit matrik logam (MMCs) mempunyai potensi besar sebagai bahan pembungkusan berbanding kumpulan-kumpulan komposit yang lain kerana sifat-

sifatnya yang boleh disesuaikan mengikut keperluan rekabentuk. Matriks kuprum yang dicampur dengan tetulang zarah silicon karbida mempunyai potensi yang lebih besar kerana ia mempunyai koduksi haba yang lebih tinggi berbanding aluminium yang digunakan secara meluas. Walaubagaimanapun, ikatan di antara matriks kuprum dan tetulang SiC perlu dipertingkatkan memandangkan terdapat masalah antara muka yang memberi kesan kepada sifat-sifat termofizikal komposit CuSiC. Oleh itu, SiC disalut dengan lapisan nipis kuprum melalui teknik salutan tanpa elektrik yang murah, mudah dan dapat memberikan salutan kuprum yang homogen. SiC disalut dengan kuprum dibawah suhu dan pH yang sesuai dalam satu larutan salutan kuprum. Kemudian komposit CuSiC difabrikasikan dengan kaedah metalurgi serbuk dengan menggunakan cara pengisaran bebola untuk mencampurkan matriks kuprum dan tetulang SiC. Campuran tersebut ditekan dibawah beban pemadatan dan disinter pada suhu 925°C selama 2 jam.

Imej SEM menunjukkan perbezaan diantara SiC asal dengan SiC yang telah dibersihkan menggunakan acetone secara ultrasonik. Selepas proses pemekaan dan pengaktifan, imej SEM menunjukkan ia mempunyai unsur-unsur pemangkin semasa proses pengaktifan. Kemudian, imej SEM selepas proses salutan kuprum menunjukkan ada deposit kuprum pada permukaan SiC. Taburan saiz zarah meningkat dari 45.639µm sebelum dibersihkan kepada 45.993µm selepas dibersihkan. Kemudian saiz zarah meningkat kepada 46.750µm selepas proses pemekaan dan pengaktifan. Kemudian saiz zarah meningkat kepada 48.100µm selepas proses salutan kuprum.

Komposit CuSiC adalah lebih ringan berbanding logam kumprum tulen. Ketumpatan bagi kuprum ialah 8.93g/cm^3. Ketumpatan bagi komposit CuSiC dengan tetulang zarah SiC bersalut kuprum adalah diantara 7.48g/cm^3 dan 3.44g/cm^3 dengan

pecahan isipadu tetulang meningkat dari 0.1, 0.2, 0.3, 0.4, 0.5, 0.6 dan 0.7. Peratusan keliangan meningkat dengan kenaikan pecahan isipadu tetulang kerana terdapat H_2 yang terperangkap semasa proses salutan zarah tetulang SiC.

ACKNOWLEDGEMENT

In the name of Allah, the Most Gracious and the Most Merciful.

Alhamdulillah, all praises to Allah for the strengths and His blessing in completing this research report. Special appreciation goes to my supervisor, Dr Ching Yern Chee, for her supervision and constant support throughout this research project.

I would like to express my appreciation to the Dean, Faculty of Engineering, and also to the Deputy Dean (Postgraduate Studies), Faculty of Engineering, for their support and help towards my postgraduate affairs. My acknowledgement also goes to all the office staffs of Postgraduate Studies, Faculty of Engineering for their co-operations.

Sincere thanks to all my friends especially En. Azmi Kamardin and En. Mohd Tajuddin Mohd Idris for their kindness and moral support during my study. Their invaluable help of constructive comments and suggestions throughout the experimental and research works have contributed to the success of this research. Thanks for the friendship and memories.

Last but not least, my deepest gratitude goes to my beloved mother, Pn. Maryam binti Abd Rahman and also to my sisters; Azima, Azifa, Afiza and Anis and my brother Anas, for their endless love, prayers and encouragement. To those who indirectly contributed in this research, your kindness means a lot to me. Thank you very much.

TABLE OF CONTENTS

ABSTRACT ii

ABSTRAK iv

ACKNOWLEDGEMENT vi

TABLE OF CONTENTS vii

LIST OF FIGURES x

LIST OF TABLES xii

CHAPTER 1 – INTRODUCTION

1.1 Background 1

1.2 Problem Statement 5

1.3 Research objectives 5

1.4 Scope of works 6

CHAPTER 2 – LITERATURE REVIEW

2.1 Advanced packaging materials 7

2.2 Metal matrix composites (MMCs) 9

2.2.1 Fabrication of MMCs 9

2.2.2 Fabrication of copper composites via Powder Metallurgical approach 12

2.3 Electroless metal deposition process 13

2.3.1 Pretreatments of nonmetallic substrates 15

2.3.2 Electroless copper deposition on SiC particles 16

CHAPTER 3 – METHODOLOGY

3.1 Raw materials 20

3.2 Electroless coating 21

3.2.1 Surface treatments 21

3.2.2 Electroless copper coating 24

3.3 Characterizations on copper coated silicon carbide particles 27

3.3.1 Scanning electron microscope (SEM) exanimation 27

3.3.2 X-ray diffraction (XRD) analysis 27

3.3.3 Particle analyzer analysis 28

3.4 Fabrication of $CuSiC_p$ composites 28

3.4.1 Preparation of green compacts 31

3.4.2 Sintering process 33

3.4.3 Density and porosity measurements 35

CHAPTER 4 – RESULTS AND DISCUSSIONS

4.1 XRD analysis on raw materials 37

4.2 Characterization of electroless coating on SiC 38

4.2.1 SiC surface treatments 38

4.2.2 Electroless copper coating 43

4.3 Fabrication of $CuSiC_p$ composites 45

4.4 Density and porosity measurement 47

CHAPTER 5 – CONCLUSION AND RECOMMENDATION

5.1 Conclusion 51

5.2 Recommendation 53

APPENDIX A

Result analysis report for particle size distribution using Malvern

Mastersizer2000 instrument.

APPENDIX B

Pycnometer results for Cu matrix reinforced with different volume fraction of Cu-coated SiC particles.

APPENDIX C

Pycnometer results for Cu matrix reinforced with different volume fraction of non-coated SiC particles.

BIBLIOGRAPHY

LIST OF FIGURES

Figure 1.1: An increase in power consumption in Intel's microprocessors (Krieg 2004).

Figure 1.2: The thermo physical properties of advanced packaging materials (Zweben 2006).

Figure 3.1: The flow chart of the whole experimental process.

Figure 3.2: Ultrasonic cleaning of SiC particles.

Figure 3.3: Filtering the SiC particles after ultrasonic cleaning in acetone for 15 minutes.

Figure 3.4: Sensitization process of SiC particles.

Figure 3.5: Activation process of SiC particles.

Figure 3.6: Oven for drying process of SiC particles.

Figure 3.7: Electroless solution bath for coating process of SiC particles.

Figure 3.8: Electroless copper coating process of silicon carbide particles.

Figure 3.9: Mold and tool set used in green compaction process.

Figure 3.10: Ball mill process of the composite powders.

Figure 3.11: Compaction process using uniaxial Gotech 200kN UTM machine.

Figure 3.12: The tube furnace for sintering process.

Figure 3.13: The temperature profile for the sintering process.

Figure 3.14: Pycnometer for true density measurement.

Figure 3.15: Density meter for bulk density measurement.

Figure 4.1: (a) XRD pattern for raw spheroidal Cu powder.

Figure 4.1, continued: (b) XRD pattern for raw SiC particles and (c) XRD pattern for CuSiC composite.

Figure 4.2: The acetone waste after SiC cleaning using ultrasonic bath.

Figure 4.3: The surface morphology of the SiC particles (a) and (b) before surface cleaning, (c) and (d) after surface cleaning, (e) and (f) after sensitizing and activation of the surface.

Figure 4.4: Particle size of the SiC particles (a) before surface cleaning, (b) after surface cleaning, (c) after sensitizing and activation of the surface.

Figure 4.5: The surface morphology of the Cu-coated SiC particles (a) at 500x magnification, (b) at 3000x magnification, and (c) at 10000x magnification.

Figure 4.6: Particle size distribution for Cu-coated SiC.

Figure 4.7: (a) Successful compaction of CuSiC with Cu-coated SiC reinforcement and (b) Unsuccessful compaction of CuSiC with non-coated SiC reinforcement at volume fraction of 0.6.

Figure 4.8: Measured density for both Cu-coated SiC and non-coated SiC reinforcement in CuSiC composites.

Figure 4.9: Bulk density for both Cu-coated SiC and non-coated SiC reinforcement in CuSiC composites.

Figure 4.10: Density measured using pycnometer for both Cu-coated SiC and non-coated SiC reinforcement in CuSiC composites.

Figure 4.11: Percentage of porosity for both Cu-coated SiC and non-coated SiC reinforcement in CuSiC composites.

LIST OF TABLES

Table 2.1: Properties of advanced materials with high thermal conductivity and low coefficient of thermal expansion (Zweben 1999 &Zweben 2005).

Table 3.1: The basic characteristics of the powders as received from manufacturers.

Table 3.2: The compositions of the electroless copper bath.

Table 3.3: The amount of Cu and non-coated SiC powders required for the CuSiC composites.

Table 3.4: The amount of Cu and $SiC_{Cu\text{-}coated}$ powders required for the $CuSiC_{Cu\text{-}coated}$ composites.

CHAPTER 1

INTRODUCTION

1.1 Background

There has been a great market demand for electronic devices and systems for the past few decades. Companiesandmarkets.com has reported on September 2011, the thermal management market is expected to grow from $6.7 billion in 2011 to $9.1 billion by 2016. More than 80% of the total thermal management market is dominated by the thermal management hardware such as heat sinks, fans and blowers. Therefore, the progress of the technology in thermal management hardware is also expected to increase due to the demands in increased functionality and miniaturization of each single device unit. It is at the same time, have increased the need for new advanced thermal management materials.

The microelectronic packaging is moving toward high density, high speed and miniaturization, as predicted by Moore's Law. The numbers of interconnections and wire length have been reduced exponentially. At the same time, the amount of power dissipation in a single device has been increased greatly as shown in Figure 1.1. These have caused critical design issues related to the requirements of thermal management, reliability, weight and cost of the electronics packaging (Zweben 2005). The conventional packaging materials cannot fulfill the material requirements of these complex designs. A high increase in the power consumption and heat dissipation also leads to the high failure rate in electronic packaging. The studies of the electronic industry have shown that, 55% of failures in electronics packaging come from temperature dependent fault (Neubauer 2005). These failures can be caused by the

temperature of the chips and the thermal expansion mismatch between the board and chip (Kowbel 2000). In order to solve these issues, varies of advanced packaging materials have been developed. The thermo physical properties of these materials are shown in Figure 1.2.

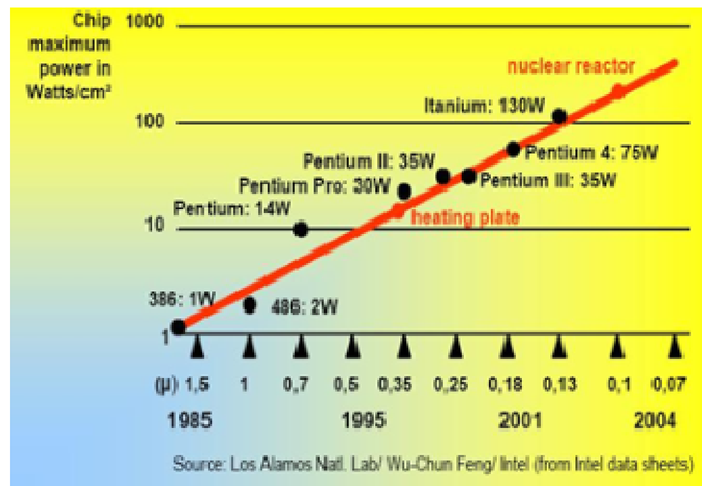

Figure 1.3: An increase in power consumption in Intel's microprocessors (Krieg 2004).

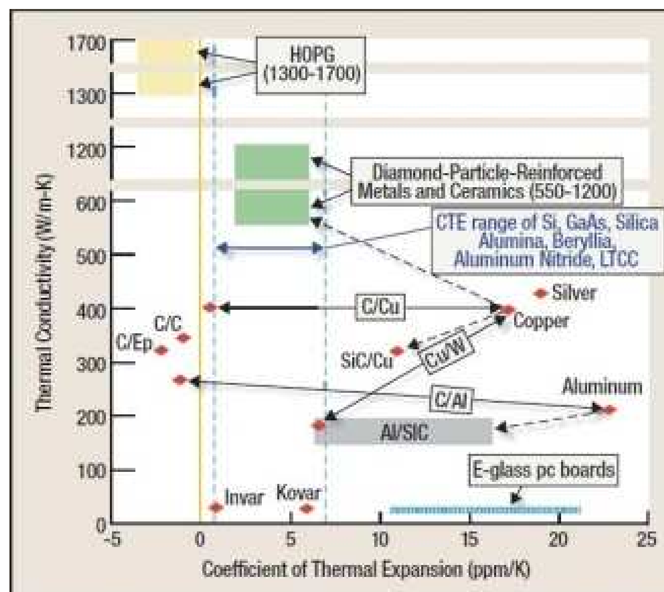

Figure 1.4: The thermo physical properties of advanced packaging materials (Zweben 2006).

Composites are the most common types of packaging materials. These advanced packaging composites can be classified into three main groups; polymer matrix composites (PMCs), carbon/carbon composites (CCCs) and metal matrix composites (MMCs) (Zweben 2005). The key reinforcements of these composites are continuous and discontinuous thermally conductive carbon fibers and thermally conductive ceramics particles such as silicon carbide and beryllium oxide. Composites those reinforced with fibers are strongly anisotropic. Where else, composites those reinforced with particles are usually isotropic.

Metal matrix composites (MMCs) have great potentials as packaging materials among the composite groups because the properties of MMCs can be engineered to meet the above design needs. The coefficient thermal expansion (CTE) of the MMCs can be altered to match the CTE of semiconductors, ceramics substrates and optical fibers by controlling the percentages of each component in the composites. Thus the thermal stresses and warpage issues can be minimized at the same time. At the time being, the most interested MMC is aluminum matrix reinforced with silicon carbide particle or Al-SiC. It is not only very cost effective thermal management material for electronics packaging (Occhionero 2005) but also performs better than copper metal (Romero 1995). The CTE of Al-SiC can be altered between 6.2 to 23 ppm/K however, its thermal conductivity is limited to 220 W/m.k. Copper, in fact has almost double the thermal conductivity of aluminum. Therefore, for heat sinks which require materials with higher thermal conductivity, copper matrix reinforced with silicon carbide particle, $Cu\text{-}SiC_p$ has a greater potential than Al-SiC.

Copper matrix reinforced with silicon carbide particles ($Cu\text{-}SiC_p$) composites and copper matrix reinforced with carbon fiber ($Cu\text{-}C_f$) composite are the most

interesting copper based MMCs in packaging materials industry. The Cu-SiC_p composites seem to have more potential as packaging materials as compared to Cu-C_f due to the anisotropic behavior of the carbon fiber. However, Cu-SiC_p system also suffers the same interface problems as in the Cu-C_f system due to the absence of bonding between the two constituents. In order to develop the Cu-SiC_p interface, the bonding between the matrix and the reinforcement phases must be improved. One of the methods to improve the bonding is by coating the reinforcement with a metal film. Coated reinforcement can produce more than 20% increase in the thermal diffusivity of the composites as compared to the non-coated ones (Neubauer 2005). Significant improvements in thermal conductivity and CTE of Cu-SiC_p composites as compared to the non-coated Cu-SiC_p composites were also observed by Shu (2003) and Schubert (2008).

There are many methods available to coat the surface of the nonmetallic reinforcements, such as sputter coating (Kock 2007; Shubert 2008), chemical vapor deposition (CVD) (Brendel 2005), physical vapor deposition (PVD) (Navinsek 1999), sol-gel coating (Torres 2007; Rams 2006) and electroless plating (Sard 1970, Chan 1999 and Chang 1996, Li 2005, Han 2006 & Sharma 2006). Among all these methods, electroless plating is the least expensive, simple and able to provide copper deposits with excellent physical and metallurgical (Deckert 2002). Moreover, a homogeneous copper film on the SiC particles can be obtained using electroless coating process to promote bonding between copper and SiC_p (Shu 2003). The improved bonding between copper coated SiC_p and copper matrix allowed applied load to be transferred more efficiently and contributed to larger strain-to-failure figures (Davidson 2000). Furthermore, these composites have relatively higher density, lower porosity and

mechanically more superior than those fabricated from uncoated powders (Moustafa 2002).

1.2 Problem statement

Copper matrix reinforced with silicon carbide particles (Cu-SiC_p) composites fabricated using powder metallurgy methods have inferior thermophysical properties due to the absence of reaction between the copper matrix and the SiC reinforcement. The bonding between the copper matrix and the SiC reinforcement must be improved in order to improve the thermophysical properties of the Cu-SiC_p composites. One of the methods to improve the bonding is by coating the SiC particles with a homogeneous copper film using electroless coating process. Numerous studies showed that a continuous copper film can be developed on the surface of SiC_p, but only a few were directly studying the effects of the electroless copper coating on the density of the $CuSiC_p$ composites. Therefore, it was substantial to fabricate the Cu-SiC_p composites by using electroless copper coating method. The properties of coated SiC in Cu-SiC_p composites can be evaluated by comparing the characteristics to those made from uncoated SiC particles.

1.3 Research objectives

The thermophysical properties of Cu-SiC_p composites can be optimized by improving the bonding between the copper matrix and SiC_p reinforcement. This can be done using an electroless coating process. With these considerations in mind and the statements made in the preceding introduction concerning the potentials of the Cu-SiC_p

composites as thermal management materials, the present work is aimed for the following objectives:

i. To prepare the copper coated SiC using electroless coating process to achieve homogenous copper deposit on the SiC particles.
ii. To fabricate the composites with different volume content of SiC particle reinforcement using powder metallurgy method.
iii. To characterize the Cu-coated SiC_p reinforcement by using XRD, SEM and particle analyzer. The density of the Cu-SiC_p composites made from copper coated SiC particles will be compared to those made from uncoated SiC powders.

1.4 Scope of works

The scope of this research is quite narrow. It consists of the electroless copper coating process of SiC particles and the fabrication process of Cu-SiC_p composites using a conventional powder metallurgical methodology. The electroless coating process that is performed in this research study is not new but rather a reproduced process which was published in numerous books and journals. However, a few modifications were made in the coating process to improve the quality of the electroless copper deposit. XRD and SEM analysis were performed to determine the homogeneity and purity of the copper film on the SiC particles. Then, the powder metallurgical methodology will be used to fabricate the Cu-SiC_p composites at different volume contents of SiC particles. The fabrication techniques involve the conventional uniaxial powder pressing and sintering processes. The experimental data are analyzed to determine the effects of volume content of non-coated SiC particles and coated SiC particles on the density of the Cu-SiC_p composites.

CHAPTER 2

LITERATURE REVIEW

2.1 Advanced packaging materials

Electronic packaging refers to the packaging of the integrated chips, interconnections, encapsulations, cooling devices, power supply and the housing (Chung 2000). Large attentions have been given to the integrated chips, resulted in a rapid increase in the packing density of devices on the chip. Thus, the amount of heat generated by each chip has increased greatly. As the power of electronics increases, the heat dissipation problem becomes even more difficult to handle. The traditional packaging materials such as Invar, Kovar, copper-tungsten and copper molybdenum have limited thermal conductivities and need to be replaced. Therefore, new advanced packaging materials have been developed.

High thermal conductivity and low thermal expansion requirements have been the driving force for the development of new advanced packaging materials. These advanced materials can be categorized into three different groups; composites, monolithic carbonaceous materials, advanced metallic alloys (Zweben 2005). Most of these advanced packaging materials are composites. Composite is a combination of two or more distinct materials, having a recognizable interface between them (Miracle & Donaldson 2001). Based on Zweben (2005), the most important packaging composites consist of carbon/carbon composites (CCCs), ceramics matrix composites (CMCs), polymer matrix composites (PMCs) and metal matrix composites (MMCs). The most typical reinforcements are continuous and discontinuous fibers and ceramic particles such as diamond, silicon carbide, beryllium oxide and graphite flakes. Carbon fiber

reinforced composites are strongly anisotropic while the particles reinforced composites tend to have isotropic properties. The properties of these advanced composites are listed in Table 2.1.

Table 2.2: Properties of advanced materials with high thermal conductivity and low coefficient of thermal expansion (Zweben 1999 & Zweben 2005).

Matrix	**Reinforcement**	**Thermal conductivity (W/m.K)**	**CTE (ppm/K)**	**Specific gravity**
CVD diamond	-	1100 – 1800	1 – 2	3.52
Highly Oriented Pyrolytic Graphite	-	1300 – 1700	-1.0	2.3
Natural graphite	-	150 – 500	-1.0	-
Aluminum	-	218	23	2.7
Copper	-	400	17	8.9
Tungsten	Copper	157 – 190	5.7 – 8.3	15 – 17
Epoxy	natural graphite	370	-2.4	1.94
Polymer	continuous carbon fibers	330	-1	1.8
Copper	discontinuous carbon fibers	300	6.5 – 9.5	6.8
Copper	continuous carbon fibers	400 – 420	0.5 – 16	5.3 – 8.2

Copper	SiC particles	320	7 – 10.9	6.6
Aluminum	graphite flake	400 – 600	4.5 – 5.0	2.3

2.2 Metal matrix composites (MMCs)

The important characteristic of MMCs is their thermal properties can be altered to required value. For example, the thermal conductivity of carbon fiber reinforced MMCs can be as high as 900 W/m.K, making them competitive to heat pipes over a short distance. Alternatively, the particles reinforced MMCs can be used as heat spreaders for highly isotropic in plane conductivities.

For electronic packaging, the matrices of MMCs can be aluminum, magnesium, cobalt, copper, and silver. The reinforcements include continuous and discontinuous carbon fibers, graphite flakes, silicon carbide (SiC), diamond, and beryllia particles. SiC particle reinforced with aluminum composite (Al-SiC) has been used widely as packaging materials for a few decades. The advantages of Al-SiC are its CTE can be as low as 6.2 ppm/K and it can be a very cost effective packaging material due to its low density. The only disadvantage of Al-SiC is its thermal conductivity is limited to 220 W/m.K. For that reason, Cu-SiC_p composites seem to have a greater potential than Al-SiC because copper has almost double the thermal conductivity of aluminum.

2.2.1 Fabrication of MMCs

MMCs can be fabricated using a wide variety of fabrication methods such as solid state, liquid state, deposition and in-situ. The solid state methods can be further

classified into diffusion bonding and powder metallurgy (PM). In diffusion bonding, metal matrix in the form of foil is consolidated with the reinforcement by applying heat and pressure. However, in PM approach, discontinuous, whisker, or particulate reinforcements are mixed with metal powders, pressed and consolidate at a temperature below the melting points of the constituents. The consolidation process can be done with or without pressure assistance. Many MMCs can be fabricated by using pressureless consolidation process via PM approach such as SiC_p reinforced copper-aluminum composites (Wang et. al. 2008).

Traditionally, the powders were compacted by using uniaxial compression techniques. The temperature of the sintering process has significant effects on the final properties of the PM products. For an example, there was a significant increase in the hardness of $CuSiC_p$ composites as the sintering temperature was increased from 900^oC to 950^oC (Celebi Efe et. al. 2011). But high sintering temperature also has negative impact to the PM products. For an example, in the fabrication of SiC_p reinforced titanium composites, the formation of silicides was observed after the samples were sintered at elevated temperature for a long time (Poletti et. al. 2008). Furthermore, a range of mechanical working methods, such as forging, rolling and extrusion, maybe applied to achieve full densification. Hot pressing method is also typically used to improve the final density of the MMCs. CuSiC composites with high vol.% of SiC_p were successfully fabricated by using a hot press method (Pelleg et. al. 1996& Schubert et. al. 2007).

In the liquid state, the reinforcements are wetted by the molten metal matrix during the consolidation process which is adapted from the conventional casting techniques. The reinforcements can be mixed with molten metal during melt stirring

process but the volume content of the reinforcement is limited to approximately 20 vol.%. Beyond this value, the dispersion of the reinforcement becomes difficult. Most of the liquid state processes involve the use of pre-form reinforcement which molten metal must infiltrate. The process can be carried out at atmospheric pressure where it relies solely on the capillary action for infiltration. The infiltration process can also be performed with the assistance of an external pressure. This type of liquid state process is called squeeze casting process. The squeeze casting process can also be employed to fabricate MMCs such as CuSiC composites (Zhu et. al. 2005),AlSiC composites (Elomari et. al. 1998) and SiC_p reinforced aluminum-copper alloy composites (Onat, Akbulut & Yilmaz 2007). However, the same interfacial problem that was observed in the pressureless infiltration process of AlSiC was also observed in the CuSiC composites which were fabricated by pressure assisted infiltration process due to the formation of Cu_3Si (Xing et. al. 2005).

In the deposition process, the reinforcement particles are mixed with atomized metal and sprayed by fine droplets. Then the metal and the substrate are co-deposited onto a substrate and left to solidify. Many available methods have been used in the fabrication of MMCs, such as chemical and physical vapor depositions, electroplating, sputtering and plasma spraying. Based on Brendelet. al. (2007), the electroplating of Cu layer on SiC fiber can be done in a copper (II) sulphate ($CuSO_4$) bath at room temperature. The effects of the electroless copper deposit on tensile strength of $CuSiC_p$ composites was studied by Davidson & Regener (2001) by pressureless sintering process. Their experimental results revealed enhanced failure strain in the Cu coated $CuSiC_p$ composites compared to their uncoated equivalents. In-situ SEM observations of the fracture process also showed improved bonding between the Cu coated SiC_p and the Cu matrix. A thin titanium layer deposited by electroplating process on the SiC

fibers can improve the tensile strength of the SiC fiber reinforced Cu composites (Luo et. al. 2007). The application of magnetron sputtering to deposit chromium and tungsten interlayers on SiC fibers were demonstrated by Kock, Brendel& Bolt (2007).

For in-situ processes, the MMCs are fabricated via the unidirectional solidification of eutectic alloys which leads to the formations of two different microstructures. Most of the time, the matrix is a solid solution and the reinforcement phase is an intermetallic compound or carbide (Matthews & Rawlings 1999). By definition, unidirectional solidified eutectics are not true composite materials. Nevertheless, they behave closely to that of composites with aligned fibers.

2.2.2 Fabrication of copper composites via PM approach

There are three main types of copper MMCs; diamond particles reinforced copper composites, carbon fiber reinforced copper composites ($Cu-C_f$), and SiC particles reinforced copper composites ($Cu-SiC_p$) (Neubauer 2005). Diamond particles reinforced copper composites are good candidates for heat sink applications due to the combination of high thermal conductivity of 640 W/m.K and low CTE of $9x10^{-6}$ K^{-1} (Schubert et. al. 2008). The thermal conductivity of diamond particles reinforced copper composites depends greatly on the volume content and particle size of the diamond particles (Yoshida & Morigami 2004). $Cu-C_f$ composites are also good candidates for packaging materials due to the combination of low CTE and weight of the carbon fiber. The CTE of $Cu-C_f$ composites can be engineered preferably by the volume content and average length of the fibers (Korb, Buchgraber & Shubert 1998). Furthermore, the CTE of $Cu-C_f$ composites can be tailored to be approximately equal to that of silicon, thus the composites can be soldered directly to the silicon wafers (Kuniya et. al. 1983). These

$Cu\text{-}C_f$ composites can be economically fabricated via conventional powder metallurgy approaches followed by a hot press process. The final properties of these $Cu\text{-}C_f$ composites suffer from the weak interface between the copper matrix and the carbon fiber reinforcement, and the inhomogeneous dispersion of carbon fibers in the copper matrix. Moreover, the properties of the $Cu\text{-}C_f$ composites are anisotropic thus they have a limited use in the thermal management application.

Due to the anisotropic behavior of $Cu\text{-}C_f$ composites, the use of SiC particles as reinforcements in copper MMCs becomes a great interest. $Cu\text{-}SiC_p$ composites can also be fabricated by using hot press process via powder metallurgical approach (Chang & Lin 1996). The CTE of $Cu\text{-}SiC_p$ composites can be tailored by controlling the volume content (Prakasan, Palaniappan & Seshan 1997) and the size of SiC_p (Elomari 1998 and Zhu et. a. 2005). But similar to $Cu\text{-}C_f$ composites, $Cu\text{-}SiC_p$ composites also suffer from similar bonding problem. In order to develop and strengthen the bond between Cu matrix and SiCp reinforcement, the bonding between the matrix and the reinforcement phases must be improved. One of the methods to improve the bonding is by coating SiC reinforcement with Cu film. With an addition of 20 vol.% of SiC, the mechanical properties of the composites can be improved three times better than pure copper (Chan & Lin 1996).

2.3 Electroless metal deposition process

The basic components for the electroless plating bath are a metal salt and a reducing agent. But most of the time, a complexing agent, stabilizers, accelerators, or inhibitors, are also required to control the rate and stability of the plating process. Furthermore, the plating process must be performed under controlled pH and

temperature. The metal salt is the source of the metal ions which during the electroless plating, is reduced by the reducing agent. The complexing agent acts as a buffer which reduces the concentration of free metal ions thus decreasing the rate of the reaction. Without the presence of the complexing agent, spontaneous precipitation of metal salt can occurs especially when the electroless plating process is performed at an elevated temperature. Besides the complexing agent, the stabilizer is also an important addition to the plating solution. It prevents the spontaneous decomposition of the plating bath due to a sudden increase of hydrogen gas during the plating process. The concentration of the stabilizer must be controlled carefully to prevent plate-out of metal on the walls of the plating tank. The temperature of the plating bath must be controlled at a certain range to prevent solution plate-out or even decomposition. The temperature of the bath is also critical in controlling the voids in the metal deposit. Large amount of voids was observed on electroless copper deposit from plating baths containing formaldehyde and glyoxylic acid as reducing agents at low temperature (Wu and Sha 2009).

The surface cleaning is critical in developing good bonding between the substrate and the metal deposit. The removal of foreign contaminants such as dirt, soil, grease and tarnish can be done by using acetone or commercial alkaline cleaners. The removal of oxide surface can be done through chemical attack or etching, acid pickling solutions and alkaline deoxidizing materials.

Electroless plating has been used extensively in many industries such as aerospace, automotive, chemical processing, oil and gas, mining and military applications. For an example, electroless nickel coatings improve inherent characteristics by adding hardness, wear resistance, corrosion protection and solderability of aluminum components in aerospace industry. In the automotive

industry, the use of electroless nickel on carburetors, fuel supply systems and fuel pumps has gained wide acceptance. Corrosion related problems in the chemical processing industries can also be minimized by means of electroless nickel coating. Oil and gas industry is also an important market due to the corrosion and wear of various drilling and piping components. Besides these industries, other applications such as molds and dyes, foundry tooling and printing industry are also taking advantages of the unique properties of the electroless plating processes.

2.3.1 Pretreatments of nonmetallic substrates

The main difference between metallic and nonmetallic substrates resides in the nature of the bond between the substrate and the metal deposits. Nonmetallic substrates require further treatments involving microetching, sensitizing and activation after surface cleaning process because the nonmetallic substrates lack of catalytic properties and therefore require activating treatment that will render them catalytic. The microetching process basically roughens the substrate surface where crater-like impressions are created. These will provide a large surface area with many sites for mechanical interlocking of the metal deposits. Then the sensitization process is applied. In this process, clusters of Sn are adsorbed onto the substrate surface in its oxidized forms (Sn^{2+} and/or Sn^{4+}) to form a continuous film. Other Sn^{2+} ions are then directly oxidized to form layers of stannic compounds over the surface (Natividad 2004). Next in the activation process, a small amount of palladium is chemically deposited on the substrate surface. The palladium acts as a catalyst for the eletcroless metal depositon to occur.

The Sn^{2+} ions will reduce the Pd^{2+} to precipitate catalytic palladium seeds on the substrate surface. The insoluble stannic hydroxide reacts with hydrochloride acid to form soluble stannous and stannic chlorides which are removed from the substrate surface via thorough rinsing process. With the exposure of the active palladium nuclei, the substrate is ready for electroless plating process.

2.3.2 Electroless copper deposition on SiC particles

The electroless copper plating techniques are mostly conducted in the fabrication of electronic parts and printed circuit boards. But recently, it has been introduced in the fabrication of metal matrix composites to improve the bonding between the metal matrix and the nonmetallic reinforcements. The theoretical basis of the electroless copper deposition has been studied and published in many papers and journals. Basically, the typical electroless copper solution contains a source of copper ions, a reducing agent, a complexant, an inhibitor, an exaltant and/or a stabilizer. Copper salts such as copper sulphate chloride or nitrate are mostly used as copper ions sources. Formaldehyde in the other hand is widely used as a reducing agent.

The presences of copper ions and a reducing agent are enough to initiate thermodynamically stable electroless copper deposition process. But in actual condition, a slight change in the pH of the solution might lead to the total precipitation of copper ions. In order to overcome this difficulty, a complexing agent is added to the solution. Complexing agents such as Rochelle salt, EDTA, glycolic acid and triethanol amine (TEA) are widely used in electroless plating baths. The possibility of using sacharose as a Cu (II) ligand in electroless copper systems has also been established (Norkus et. al. 2007). These complexing agents depress the concentration of free copper ions thus stabilize the pH of the solution during the electroless plating process. Each complexing

agent has different effect on the reduction rate of Cu(II) ions and the oxidation rate of formaldehyde (Lin & Yen 2001). The presence of complexing agents therefore has profound effects on the structure of the metal deposit. However, the selection and concentration of the complexing agent must be considered very carefully to ensure sufficient free copper ions are available for the electroless plating process.

With the presence of complexing agent in the plating solution, the plating rate will be lowered. A small addition of exaltants or accelerators will increase the plating rate without causing any instability to the plating bath. For an example, a small addition of ammonia accelerates effectively the autocatalytic reduction of Cu (II) ions by formaldehyde in EDTA solution (Vaskelis et. al. 2007). Another critical parameter to consider is the pH of the solution. The formation of byproducts such as hydrogen (H^+) or hydroxyl (OH^-) ions will change the pH of the solution during the copper deposition process. The dependence of the change in OH^- concentration on the rate of the catalytic process is markedly influenced by the rate of H_2 evolution (Valkelis 1987). Nonetheless, the presence of hydrogen has insignificant effects on the mechanical properties of the copper deposit because the solubility of hydrogen in copper is very small (Nakahara 1988). In order to stabilize the pH of the solution, buffers such as carboxylic acids are added into the solution. The addition of 2-MTB in tartarate and EDTA based plating baths also increase the copper plating rate (Hanna et. al. 2003). Other stabilizers such as 2,2'-dipyridyl has inhibiting effects on the electroless metal deposition. It increases the potential of the reduction reaction thus reducing the copper deposition rate (Li et. al. 2004). The presence of potassium ferrocyanide ($K_4Fe(CN)_6$) in the plating bath promotes defects free and smooth copper surface (Veleva 1986) which is preferred in most practical application in electronics industry (Norkus 2006). Cyanide ions are likely to adsorb strongly on copper surface and facilitate the desorption of hydrogen gas from

the deposit surface, thus promote the ductility of the copper deposits (Nakahara & Okinaka 1983). Some additives are also required to suppress the spontaneous oxidation reaction in the plating solution to prevent a very coarse and poor adhesive copper film from being developed (Oh & Chung 2006). However, the stabilizer must not be used excessively because too much stabilizers will totally shield the substrate surface and prevent the copper deposition from happening. At 10 mM concentration, most of the strong inhibitors caused a complete inhibition of the copper deposition (Bielinski 1987).

Most electroless copper solutions employ formaldehyde as the reducing agent. The reduction potential and the rate of oxidation are strongly dependent to the pH of the solution. For practical electroless copper deposition, the pH of the plating bath should be above 11. This pH restriction imposes the use of complexed copper ions in order to prevent the precipitation of copper (II) hydroxide. Furthermore, the additives also show significant effects on the cathodic reduction of the copper ions. The effects can be accelerating or inhibiting, depends on the type and concentration of the additive.

The bonding formed via electroless copper deposition process is not of an atomic nature because chemical bonding cannot be formed between the metal deposit and the nonmetallic substrates. Therefore there is only mechanical bonding exists between the metal deposit and the nonmetallic substrate.

CHAPTER 3

RESEARCH METHODOLOGY

This study concentrates on preparing the electroless copper coating on silicon carbide particles (SiC_p) and fabricate the copper matrix reinforced with copper coated silicon carbide particles ($CuSiC_p$) and non-coated silicon carbide particles composites. Then the effects of such coating on the final density and microstructure of the fabricated Cu-SiC_p composites is studied.

The experimental activities are divided into three major stages as shown in Figure 3.1. In the first stage, an electroless metal coating technique was carried out to coat SiC_p with thin copper film. Then in the second stage, $CuSiC_p$ composites were fabricated with varying volume fractions of SiC using the conventional powder metallurgical methodology. Finally in the third stage, the physical and microstructural characterization of the composites was performed. The effects of the electroless copper coating on the final density of the composites were investigated. Microstructural analysis was conducted to study the copper coating on the SiC_p and the composites. Throughout the experimental work, different methods and tests were used.

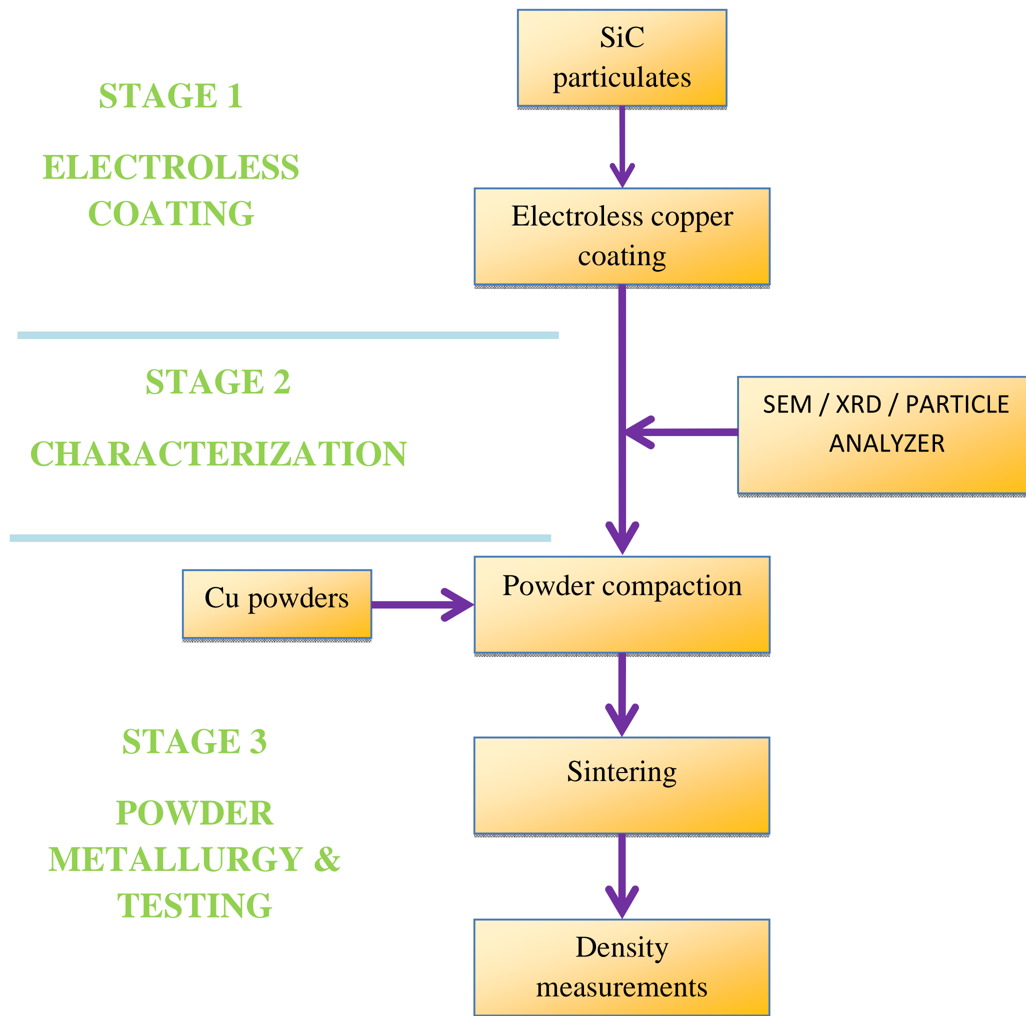

Figure 3.1: The flow chart of the whole experimental process.

3.1 Raw materials

The raw materials which were utilized for the experiments were angular shaped abrasive grade silicon carbide (SiC) powder from PRESI and 99% purity spheroidal copper (Cu) powder from Sigma Aldrich. Table 3.1 shows the characteristics of the raw materials received, as reported by the respective manufacturers.

Table 3.1: The basic characteristics of the powders as received from manufacturers.

Properties	**Unit**	**Silicon carbide PRESI**	**Copper powder Sigma Aldrich**
Particle shape	-	Angular	Spheroidal
Purity	%	-	99
Crystal structure	-	-	FCC
Particle size, D_{50}	µm	45.6	-

3.2 Electroless coating

3.2.1 Surface treatments

The cleanliness surface of the SiC particle is critical to ensure flawless Cu deposition during the electroless coating process. The treatments used to prepare the surface of SiC particles are generally similar to those used for the preparation of base metals in electroplating process. In order to obtain a homogeneous copper deposit on the surface of the SiC particles, the following steps were carried out:

First, 20g of SiC particles was cleaned using Ultramet 2003 Sonic Cleaner Buehler ultrasonic bath in 400ml of industrial grade acetone for 15 minutes as shown in Figure 3.2. Then the SiC particles were filtered by using Whatman® qualitative grade 4 (20-25 µm) filter papers as in Figure 3.3. The cleaning process was repeated three times.

Then, the clean filtered silicon carbide particles were dried in the oven at 75°C for 4 hours.

Figure 3.2: Ultrasonic cleaning of SiC particles.

Figure 3.3: Filtering the SiC particles after ultrasonic cleaning in acetone for 15 minutes.

After the cleaned SiC particles completely dry, the particles were etched in a diluted solution of nitric acid (65%) for 30 minutes using ultrasonic bath. Then, the SiC

particles were rinsed with 500ml of deionized water for three times. Next, the SiC particles were sensitized in a solution containing 40ml of hydrochloric acid (37%), 10g of tin (II) chloride dehydrate ($SnCl_2$) and 1000ml of deionized water. The sensitization process was performed at 40^oC for 2 hours as in Figure 3.4. The solution was continuously stirred. Then, the SiC particles were slowly rinsed with 1000ml of deionized water.

Figure 3.4: Sensitization process of SiC particles.

After rinse, the SiC particles were activated in a solution containing 1000ml of deionized water, 3ml of hydrochloric acid (37%) and 0.25g of palladium (II) chloride ($PdCl_2$). The activation process was performed at 40^oC for 1 hour under continuous stirring condition as in Figure 3.5. Then, the SiC particles were slowly rinsed with 1000ml of deionized water for three times to prevent contamination of the solution. Finally the activated SiC particles were dried in the oven at 85^oC for 4 hours as shown in Figure 3.6.

Figure 3.5: Activation process of SiC particles.

Figure 3.6: Oven for drying process of SiC particles.

3.2.2 Electroless copper coating

The electroless coating bath was prepared and the compositions of the bath solution are presented in Table 3.2. First, 2000ml of deionized water was poured into

the beaker. The deionized water was heated to 55^oC before 20g of copper (II) sulphate pentahydrate ($CuSO_4.5H_2O$) was added into the beaker. Then 66.6g of ethylenediaminetetraacetic (EDTA) acid disodium salt-2-hydrate ($C_{10}H_{14}O_8N_2Na_2.2H_2O$) was added into the solution as a complexing agent. The solution was continuously stirred by using a magnetic stirrer. The solution is heated further until it reached 60^oC. Next, 40mg of 2,2'-dipyridyl ($C_{10}H_8N_2$), 120mg of potassium hexacyanoferrate (II) ($K_4Fe(CN)_6.3H_2O$), and 23ml of formaldehyde (HCOH) 37% solution were added into the electroless coating bath solution. The solution temperature is controlled manually by adjusting the heater knob while monitoring the temperature using thermometer. The solution is shown in Figure 3.7.

Table 3.2: The compositions of the electroless copper bath.

Chemicals	**Chemical formula**	**Quantity**
Copper (II) sulphate pentahydrate	$CuSO_4.\ 5H_2O$	20g
EDTA	$C_{10}H_{14}O_8N_2Na_2.2H_2O$	66.6g
2,2'-Dipyridyl	$C_{10}H_8N_2$	40mg
Potassium hexacyaneferrate (II)	$K_4Fe(CN)_6.3H_2O$	120mg
Formaldehyde (37%)	HCOH	23ml
Sodium hydroxide solution	NaOH	up to pH 12 to 13

Figure 3.7: Electroless solution bath for coating process of SiC particles.

After that, by using a small pump, air was bubbled into the solution. The pH of the electroless coating bath was adjusted in between 12 to 13 by adding sodium hydroxide (NaOH) solution. Then, the temperature of the bath was increased to 75°C. When the temperature reached 75°C, 15g of activated SiC particles was put into the bath and the electroless Cu deposition would occurs immediately as shown in Figure 3.8. The electroless coating process were performed for 30 minutes with the temperature maintained at 75°C and the pH of the electroless bath maintained in between 12 to 13. After the coating process was completed, the Cu coated SiC particles were slowly rinsed with 400ml of hot water that was heated at 75°C. The rinsing process was repeated for five times to remove all contaminations. Then, the Cu coated SiC particles were rinsed again with 500ml of acetone twice and left to dry under room temperature. Finally the coated silicon carbide particles were dried in a tube furnace at 600°C for 2 hours under argon atmosphere.

Figure 3.8: Electroless copper coating process of silicon carbide particles.

3.3 Characterizations on copper coated silicon carbide particles

3.3.1 Scanning electron microscope (SEM) examination

The surface structure of the raw, cleaned, sensitized, activated and coated silicon carbide particles were examined by using JEOL JSM-6460LA scanning electron microscope (SEM).

3.3.2 X-ray diffraction (XRD) analysis

X-ray diffraction (XRD) analysis was performed on the purchased SiC particles. The analysis was done by using Shimadzu XRD-6000 x-ray diffractometer.

3.3.3 Particle analyzer analysis

The mean particle size, D_{50} and the particle size distribution were performed on the cleaned, sensitized, activated and Cu coated SiC particles. The analysis was done using of Malvern Mastersizer2000 particle size analyzer.

3.4 Fabrication of $CuSiC_p$ composites

The Cu powder was mixed with different volume fractions of SiC powder (v_{SiC}): 0.1, 0.2, 0.3, 0.4, 0.5, 0.6 and 0.7. The v_{SiC} is defined as the ratio of the volume of the SiC powder V_{SiC} to the volume of CuSiC composite (V_{CuSiC}). The volume fraction of Cu powder is also defined the same way.

$$v_{SiC} = \frac{V_{SiC}}{V_{CuSiC}} \quad \text{and} \quad v_{Cu} = \frac{V_{Cu}}{V_{CuSiC}}$$

where V_{Cu} is the volume of Cu powder. The volume of the CuSiC composite, V_{CuSiC} was calculated based on a cylindrical green-compact with 11mm diameter and 10mm thickness, which is theoretically equivalent to $0.95cm^3$. It was noted that

$$v_{SiC} + v_{Cu} = 1 \text{ and } V_{SiC} + V_{Cu} = V_{CuSiC}$$

The weight fraction of SiC powder (w_{SiC}) and Cu powder (w_{Cu}) are defined as the ratio of the weight of the constituents to the weight of the CuSiC composite (W_{CuSiC}).

$$w_{SiC} = \frac{W_{SiC}}{W_{CuSiC}} \text{and} w_{Cu} = \frac{W_{Cu}}{W_{CuSiC}}$$

It was noted that

$$w_{SiC} + w_{Cu} = 1 \; and \; W_{SiC} + W_{Cu} = W_{CuSiC}$$

Since v and W are related to density (ρ) as follow

$$\rho V = W$$

Therefore $$\rho_{CuSiC}V_{CuSiC} = \rho_{Cu}V_{Cu} + \rho_{SiC}V_{SiC}$$

$$\rho_{CuSiC} = \rho_{Cu}\frac{V_{Cu}}{V_{CuSiC}} + \rho_{SiC}\frac{V_{SiC}}{V_{CuSiC}}$$

$$\rho_{CuSiC} = \rho_{Cu}v_{Cu} + \rho_{SiC}v_{SiC}$$

where ρ_{CuSiC},ρ_{Cu} and ρ_{SiC} are the density of the CuSiC composite, Cu powder and SiC powder respectively. The weight fraction of SiC powder (w_{SiC}) can therefore be related to its volume fraction as the following.

$$w_{SiC} = \frac{W_{SiC}}{W_{CuSiC}} = \frac{\rho_{SiC}V_{SiC}}{\rho_{CuSiC}V_{CuSiC}} = \frac{\rho_{SiC}}{\rho_{CuSiC}}v_{SiC}$$

In the same way, the weight fraction of Cu powder (w_{Cu}) is also given by

$$w_{Cu} = \frac{W_{Cu}}{W_{CuSiC}} = \frac{\rho_{Cu}V_{Cu}}{\rho_{CuSiC}V_{CuSiC}} = \frac{\rho_{Cu}}{\rho_{CuSiC}}v_{Cu}$$

Since the volumes of the CuSiC composites were fixed at 0.95cm^3, the values for W_{Cu} and W_{SiC} for the CuSiC composites at different volume fractions of SiC powder are given in Table 3.3.

Table 3.3: The amount of Cu and non-coated SiC powders required for the CuSiC composites.

v_{SiC}	ρ_{CuSiC}	W_{SiC}	W_{Cu}	W_{CuSiC}
0.0	8.93	0.0000	8.9314	8.9314
0.1	8.36	0.3223	8.0378	8.3601
0.2	7.79	0.6436	7.1447	7.7883
0.3	7.22	0.9654	6.2518	7.2172
0.4	6.64	1.2873	5.3586	6.6459

0.5	6.07	1.6093	4.4653	6.0746
0.6	5.50	1.9306	3.5729	5.5035
0.7	4.93	2.2528	2.6794	4.9322

However, for the Cu coated SiC particles ($SiC_{Cu\text{-}coated}$), the volume of the Cu deposit on the SiC particles (V_x) is considered as a fraction of the total volume of Cu in the Cu-coated CuSiC ($CuSiC_{Cu\text{-}coated}$) composites. For that reason, the weight fraction of Cu in the $SiC_{Cu\text{-}coated}$ (w_c) must be determined prior to green compact preparation. Knowing the value of w_c, the required weight of $SiC_{Cu\text{-}coated}$ (W_y) and the required weight of Cu powder (W_x) can be calculated by the using the following equations:

$$W_{SiC} = W_y - w_c W_y$$

$$W_{Cu} = W_x + w_c W_y$$

where $w_c W_y$ is the weight of Cu deposit on the SiC particles. Both equations are only valid if the value of $W_x \geq 0$. At $W_x = 0$, the value of W_{Cu} is solely contributed by the Cu deposit on the SiC particles. In the case of $V_{CuSiC} = 0.95\text{cm}^3$ and $w_c = 0.25$, the values for W_y and W_x for $CuSiC_{Cu\text{-}coated}$ composites at different volume fractions of SiC powder are given in Table 3.4.

Table 3.4: The amount of Cu and $SiC_{Cu\text{-}coated}$ powders required for the $CuSiC_{Cu\text{-}coated}$ composites.

v_{SiC}	ρ_{CuSiC}	W_{SiC}	W_{Cu}
0.0	8.93	0.0000	8.9307
0.1	8.36	0.4293	7.9308
0.2	7.79	0.8584	6.9307

0.3	7.22	1.2876	5.9296
0.4	6.64	1.7169	4.9292
0.5	6.07	2.1456	3.9296
0.6	5.50	2.5743	2.9293
0.7	4.93	3.0037	1.9285

3.4.1 Preparation of green compacts

The weight of SiC and Cu powders are determined theoretically based on the same compact volumes as in Table 3.3 and Table 3.4. Figure 3.9 shows the mold set used in green compaction process.

Figure 3.9: Mold and tool set used in green compaction process.

The weighted Cu and SiC powders are placed in a customized milling container. Ball milling method was used using Zirconia balls with diameter of 10mm to mix both powders slowly at a fixed speed for 10 minutes as in Figure 3.10. The milling speed and

milling time were determined through try-and-error method to obtain the homogeneity mixing of both powders.

Figure 3.10: Ball mill process of the composite powders.

After the milling process, the powders were uniaxial compressed in a tool steel mold with inner diameter of 12mm under 50kN of load. Gotech 200kN UTM machine was used to perform the compaction process. The compaction process is shown as in Figure 3.11. After the compaction process, the weight, diameter and thickness of the green compacts composites were measured by using an analytical balance and a digital vernier caliper. Then the green density of each compact was calculated.

Figure 3.11: Compaction process using uniaxial Gotech 200kN UTM machine.

3.4.2 Sintering process

The green compacts composites were sintered in the furnace at 925°C for 2 hours in an argon atmosphere. In order to control precisely the heating rate, sintering temperature and cooling rate during the sintering process, VT tube furnace was used as shown in Figure 3.12. The temperature of the furnace was raised slowly at 5°C per minute to prevent thermal shock and minimize temperature gradient on the samples.

Figure 3.12: The tube furnace for sintering process.

The sintering temperature profile is shown in Figure 3.13. Once the sintering process was completed, the final mass and volume of the samples were measured again.

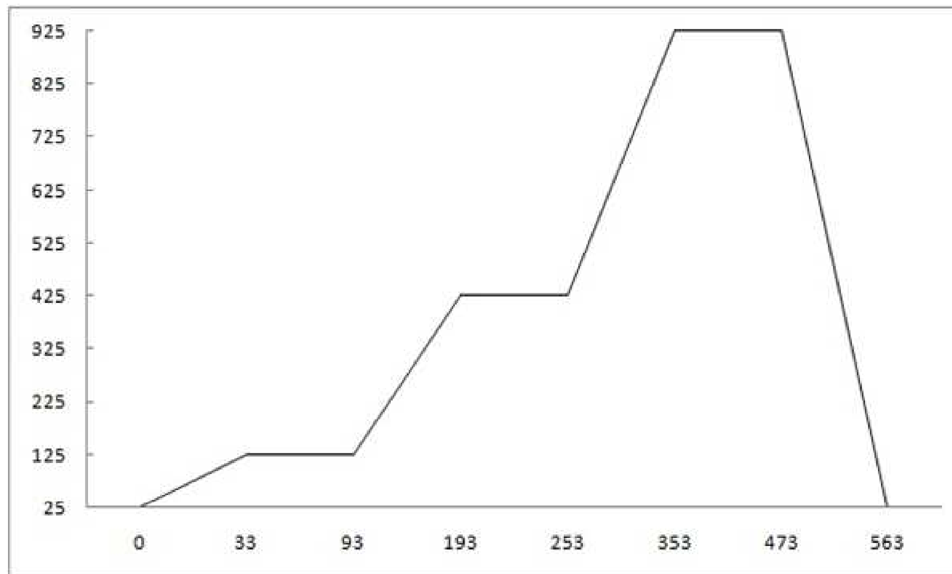

Figure 3.13: The temperature profile for the sintering process.

3.4.3 Density and porosity measurements

The true densities of the specimens were measured in a Micromeritics AccuPyc II 1340 pycnometer as shown in Figure 3.14. The pycnometer uses helium gas to measure the volume of the specimen accurately. The sample was sealed in the specimen compartment and then helium gas was passed into the compartment. Then, the pressures before the expansion and after the expansion were measured. Then, the volume of the sample was computed. The gas displacement density of the sample was then calculated by dividing the sample weight to this volume. The average true density of the composite was given by pycnometer calculation.

Figure 3.14: Pycnometer for true density measurement.

The bulk density can be obtained by measuring the specimens using density meter as shown in Figure 3.15. The difference between bulk density and true density will give the porosity percent in the specimens.

Figure 3.15: Density meter for bulk density measurement.

CHAPTER 4

RESULTS AND DISCUSSION

4.1 XRD analysis on raw material

The raw material received from the manufacturer was verified using X-ray diffraction analysis. The XRD was performed on raw Cu powder and also the raw SiC particles which later used as reinforcement in the CuSiC composites. Figure 4.1 (a) shows the XRD peaks for Cu powder which gives the crystal structure of FCC Cu powder. Figure 4.1 (b) shows the peak for raw SiC. In Figure 4.1 (c), the XRD was performed on a CuSiC composite specimen to verify the existence of both constituents in the sample. It shows both peak of Cu powder and SiC particles, which it proves that both materials exist in the composite and they behave themselves as described by the term of metal matrix composites (MMCs). This XRD result also proves that the copper coated SiC_p were free of contaminants because they were dissociated from the SiC_p surface through vigorous stirring of the electroless bath and repeated rinsing process.

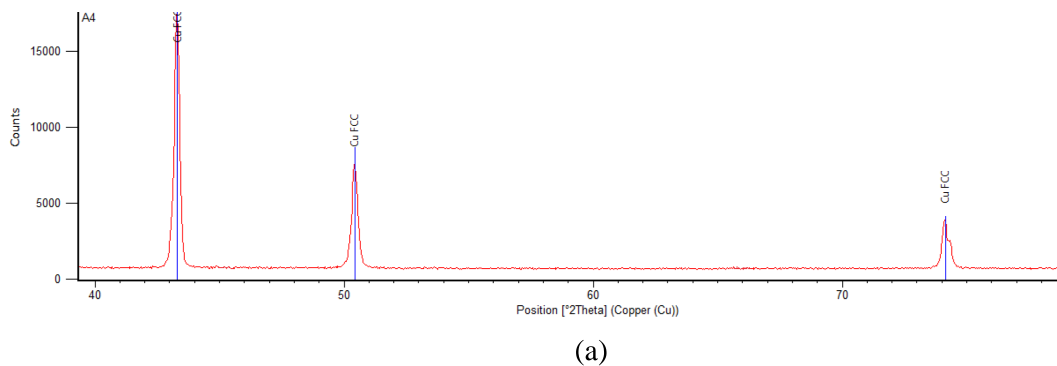

(a)

Figure 4.1: (a) XRD pattern for raw spheroidal Cu powder.

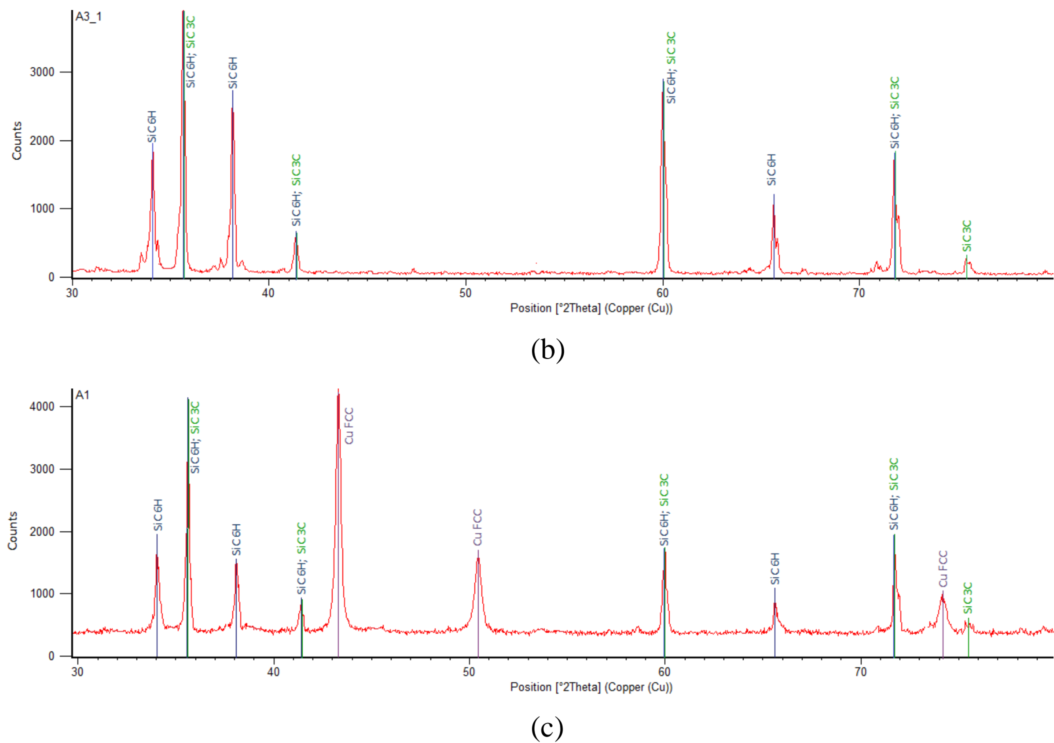

(b)

(c)

Figure 4.1, continued: (b) XRD pattern for raw SiC particles and (c) XRD pattern for CuSiC composite.

4.2 Characterization of electroless coating on SiC

4.2.1 SiC surface treatments

The bonding between the nonmetallic SiC surfaces and the Cu coating is only mechanical in nature (Mallory & Hajdu 1990). In order to achieve good adhesion of Cu deposit on surface of the SiC particles, the SiC particles were cleaned in acetone using ultrasonic bath. The solvent helps in the dissolution of the unwanted contaminants on the surface of the SiC particles. The ultrasonic cleaning uses sound waves passed at a very high frequency through the acetone, which create an active scrubbing action on the surface of the SiC particles. The cleaning process was repeated for a few times until there is no significant difference in the turbidity of the acetone waste. In Figure 4.2, it is

shown that after the third time cleaning, the acetone waste shows no significant difference. Therefore, the cleaning process was only repeated three times.

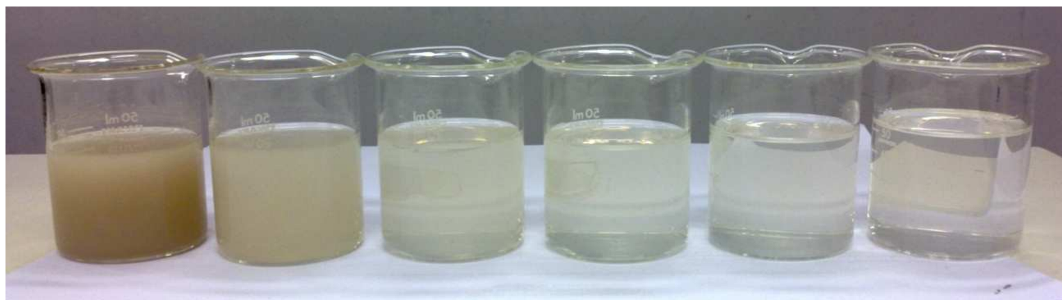

Figure 4.2: The acetone waste after SiC cleaning using ultrasonic bath.

Figure 4.3 (a) and (b), show the surface morphology for the raw SiC particles at 500x magnification and 10,000x magnification respectively. Under higher magnification, it was clearly seen the unwanted contaminants on the particle surface. After cleaned the SiC with acetone solvent, the surface morphology was again inspected under SEM. Figure 4.3 (c) and (d) show the cleaned SiC particle under 500x magnification and 10,000x magnification respectively. The surface of the SiC was cleaned from any unwanted contaminant particles and this cleaning process has rubbed away any contaminants less than 10microns.

Since Cu deposits were mechanically bonded to the surface of the SiC particles, it is important to obtain the right topography on the surface of the SiC particles. A solution of nitric acid was used to roughen the surface of SiC particles, thus improve the chances for surface attachment of the catalytically palladium metal. The nonmetallic SiC particles require activating treatments that will render them catalytic since they are lack of catalytic properties. The activation process was done by seeding the surface of the SiC particles with a catalytically active palladium metal. Figure 4.3 (e) and (f) show

the surcease of SiC after sensitizing and activation process at 500x magnification and 10,000x magnification respectively.

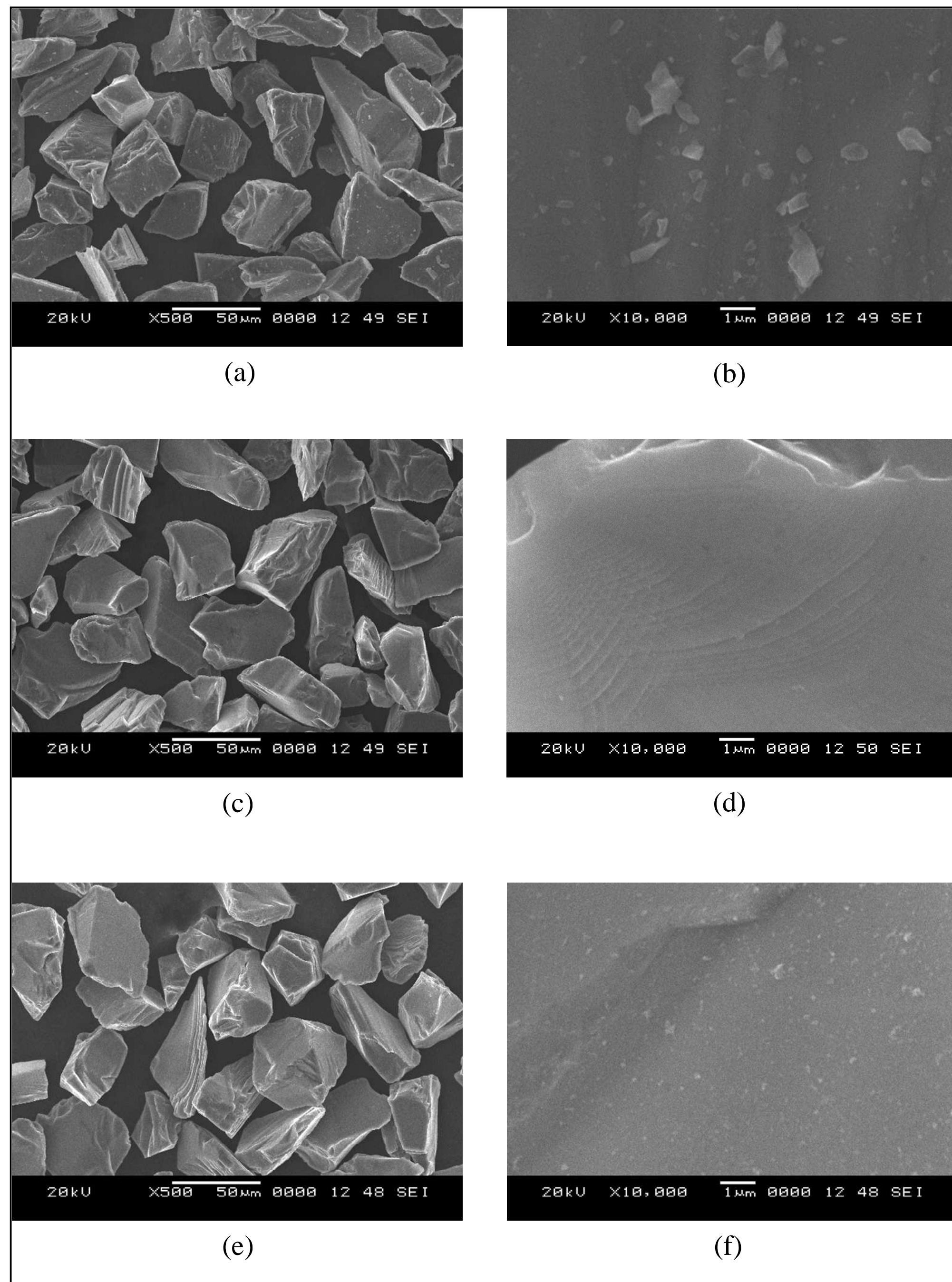

Figure 4.3: The surface morphology of the SiC particles (a) and (b) before surface cleaning, (c) and (d) after surface cleaning, (e) and (f) after sensitizing and activation of the surface.

The effectiveness of the cleaning process can also be shown by comparing the particle size distribution of SiC particles before and after the cleaning process. Figure 4.4 (a) shows the particle size distribution for the raw SiC as received from the manufacturer. The mean particle size (D_{50}) gives 45.693μm size. Figure 4.4 (b) shows that, after SiC was ultrasonically cleaned in acetone, any particles with size less than 10 micron have been successfully filtered and removed. After the cleaning process, the particle size distribution has been slightly shifted to the right where mean particle size (D_{50}) of the SiC particles has increased from 45.639μm to 45.993μm. However, the change in the particle size distribution, should be considered as a change in the particle size. The sizes of the SiC particles remain the same after the cleaning process. Only a portion of the population of the SiC particles has been removed during repeated cleaning and filtration processes. Figure 4.4 (c) shows the particle size distribution for SiC after sensitizing and activation process. The mean particle size (D_{50}) has increased to 46.750μm after the SiC surface has been seeding with a catalytically active palladium metal.

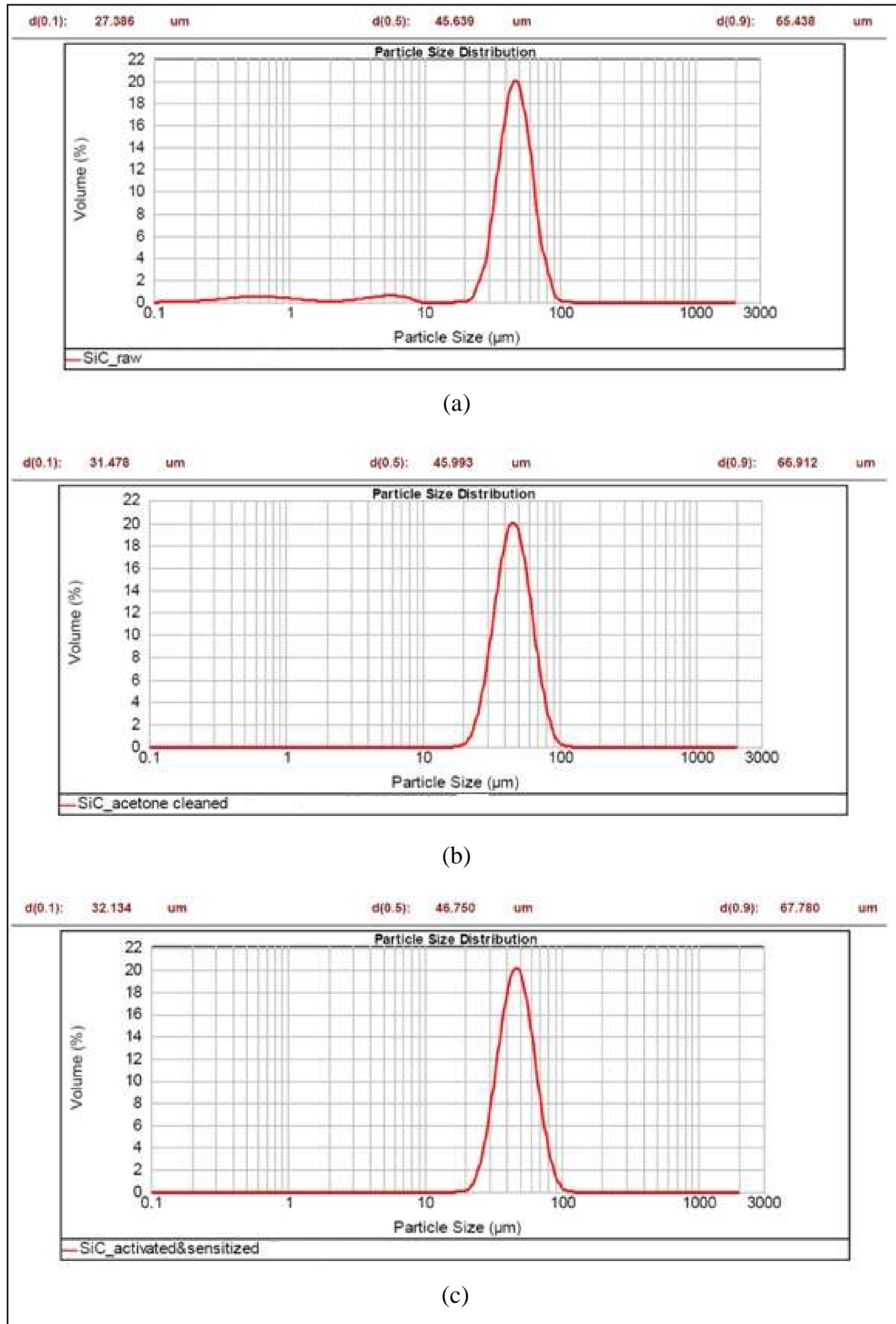

Figure 4.4: Particle size of the SiC particles (a) before surface cleaning, (b) after surface cleaning, (c) after sensitizing and activation of the surface.

4.2.2 Electroless copper coating

The two step electrochemical mechanisms occur simultaneously on the activated surface:

1. Anodic oxidation of formaldehyde

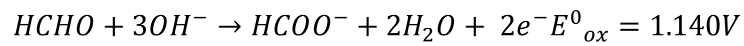

$$HCHO + 3OH^- \rightarrow HCOO^- + 2H_2O + 2e^- E^0{}_{ox} = 1.140V$$

2. Cathodic reduction of Cu ions

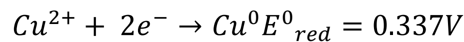

$$Cu^{2+} + 2e^- \rightarrow Cu^0 E^0{}_{red} = 0.337V$$

where $E^0{}_{ox}$ and $E^0{}_{red}$ are the standard potential energy. Therefore, the overall reaction of the electroless Cu deposition in formaldehyde-based plating solution is

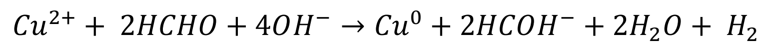

$$Cu^{2+} + 2HCHO + 4OH^- \rightarrow Cu^0 + 2HCOH^- + 2H_2O + H_2$$

The electroless Cu deposition is a thermodynamically favorable reaction since the sum E^0 of the standard potential energy of anodic and cathodic is positive, and the change in the free energy is negative since $\Delta G^0 = -nFE^0$. The spontaneous solution decomposition does not occur because the electroless Cu deposition reaction is kinetically inhibited (Diamand 1995). For Cu deposition to occur, the potential energy of the reducing agent has to be more negative than that for the metal being deposited. The potential energy for oxidation half reaction becomes more negative when the pH of the electroless solution is increased (Oita 1997).

Figure 4.5 (a), (b) and (b) show the surface morphology of SiC deposited with thin Cu after the electroless coating process under 500x magnification, 3,000x magnification and 10,000x magnification respectively.

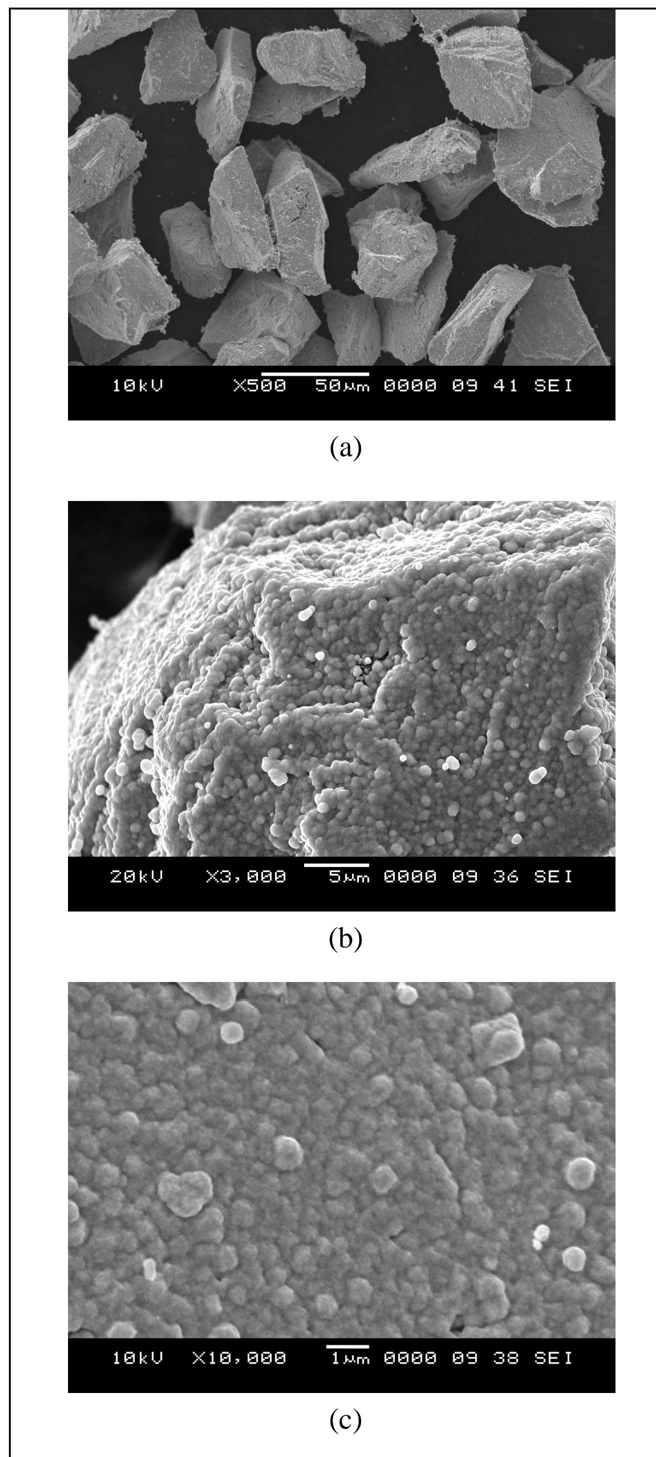

Figure 4.5: The surface morphology of the Cu-coated SiC particles (a) at 500x magnification, (b) at 3000x magnification, and (c) at 10000x magnification.

The completed Cu deposition on SiC particles after the electroless coating process was verified using the particle size distribution. Figure 4.6 shows the morphology images after SiC was deposited with thin layer of Cu. After the electroless coating process, the particle size distribution has been shifted to the right where mean particle size (D_{50}) of the Cu-coated SiC particles has increased from 46.750μm size after the sensitizing and activation process to 48.100μm. The change in the particle size distribution is due to the fact that a thin Cu film deposited on the SiC particles completely. The difference of the particle size gives a rough thickness coating of the Cu. However, the actual Cu coating thickness is best determined using measurement under SEM.

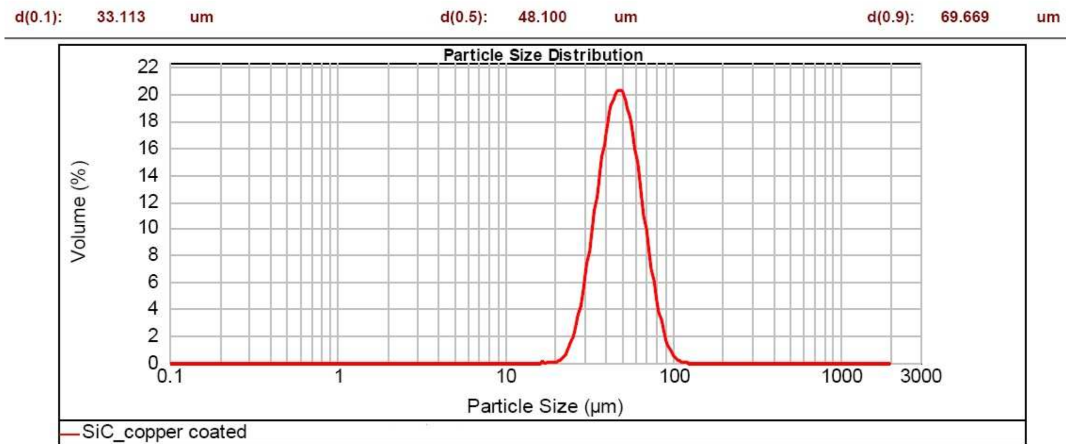

Figure 4.6: Particle size distribution for Cu-coated SiC.

4.3 Fabrication of $CuSiC_p$ composites

During preparing the mixture of composites, ball milling method was used where the speed and duration of mixing were fixed for each composite composition. Then the mixture was placed into a customized mold and tool for uniaxial compaction process. The load used for all specimens was 50kN. This conventional powder

metallurgy technique was performed for both $CuSiC_{Cu\text{-}coatedSiC}$ and $CuSiC_{non\text{-}coatedSiC}$ under different composition for comparisons.

The compaction was successful for all CuSiC composites with the Cu-coated SiC reinforcement with volume fractions: 0.1, 0.2, 0.3, 0.4, 0.5, 0.6 and 0.7. It was due to a good improved interface bonding between Cu matrix and Cu-coated reinforcement of SiC as shown in Figure 4.7 (a). However, for CuSiC composites with non-coated SiC reinforcement, the compacted specimen starts to chip and porous when volume fraction of non-coated SiC reach 0.5 due to the poor interface bonding between the two constituents as shown in Figure 4.7 (b). Therefore, for CuSiC with non-coated SiC reinforcement composites, the samples can only be obtained for volume fraction 0.1, 0.2, 0.3 and 0.4.

(a)

(b)

Figure 4.7: (a) Successful compaction of CuSiC with Cu-coated SiC reinforcement and (b) Unsuccessful compaction of CuSiC with non-coated SiC reinforcement at volume fraction of 0.6.

4.4 Density and porosity measurement

According to the overall reaction of the electroless Cu deposition in formaldehyde-based plating solution equation, the deposition of one mole of Cu is accompanied by the evolution of one mole of hydrogen (H_2). This results in the incorporation of H_2 gas bubbles into the Cu deposit. The small H_2 gas bubbles (20-300A) are incorporated uniformly throughout the copper film while the large (25-30 μm) bubbles are trapped at the grain boundaries (Nakahara & Okinaka 1983). Thus, the density of the electroless copper is expected to be lower than that of bulk copper due to the presence of incorporated hydrogen.

The measured density of CuSiC composites were done by measuring the weight, diameter and thickness of each specimen using an analytical balance and vernier caliper. As the volume fraction of SiC reinforcement increase, the density of the specimen decreases. Figure 4.8 shows the measured density for both composites with Cu-coated SiC reinforcement and non-coated SiC reinforcement. When the volume fraction of Cu matrix increases, while the volume fraction of SiC reinforcement decreases, the density is in increasing trend. The same trend can be seen in Figure 4.9 for bulk density measurement of the specimens using density meter. In this method, the specimens were weighted in air and also in water. Then, the weight of specimen in air will be divided with the volume obtained through the difference reading of mass in air and mass in water and it will give the bulk density value for each specimen.

$$\text{volume} = \text{mass}_{\text{air}} - \text{mass}_{\text{water}}$$

$$\text{density} = \frac{\text{mass}_{\text{air}}}{(\text{mass}_{\text{air}} - \text{mass}_{\text{water}})}$$

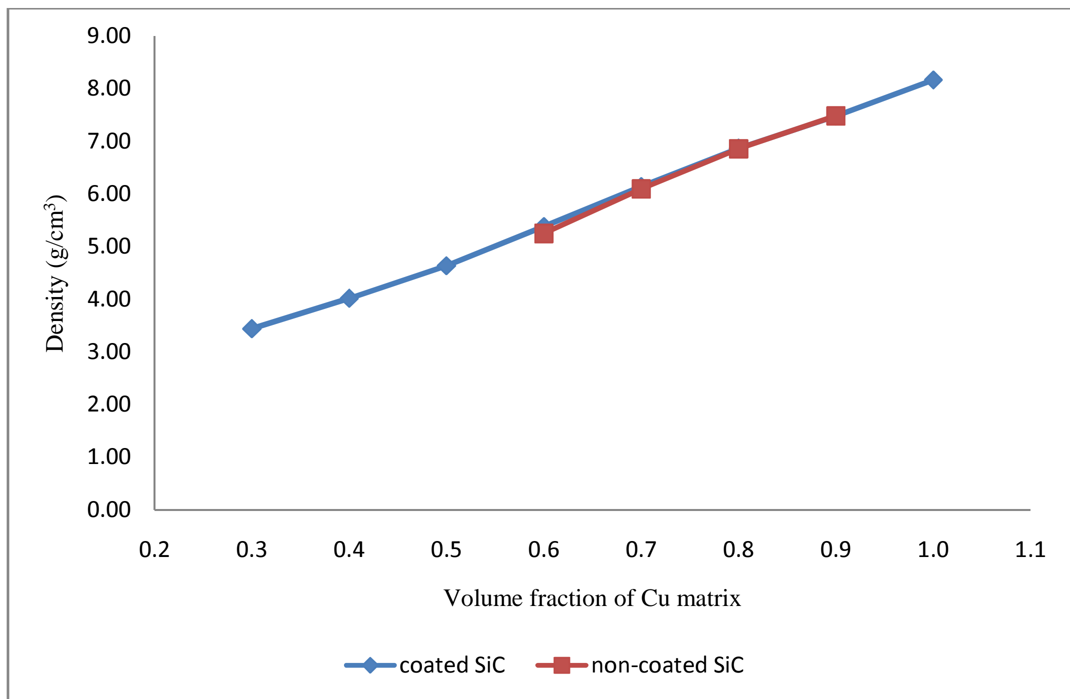

Figure 4.8: Measured density for both Cu-coated SiC and non-coated SiC reinforcement in CuSiC composites.

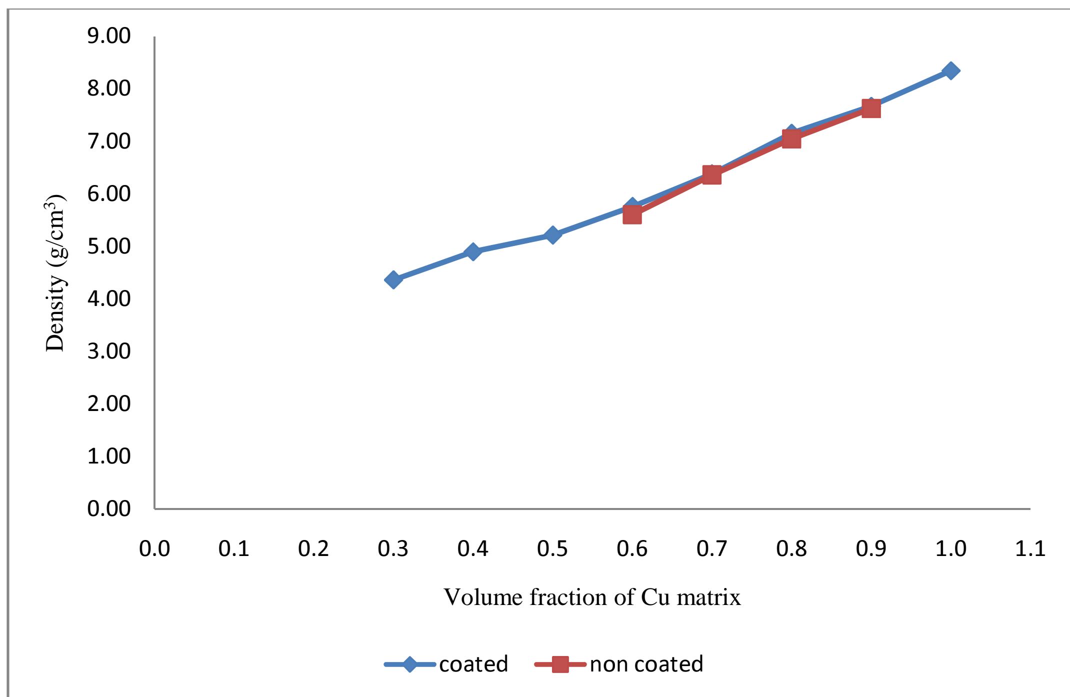

Figure 4.9: Bulk density for both Cu-coated SiC and non-coated SiC reinforcement in CuSiC composites.

The true density is obtained by using a Micromeritics AccuPyc II 1340 pycnometer. Figure 4.10 shows the increasing of density value when the volume fraction of Cu matrix increase, which the volume fraction of SiC reinforcement decreased.

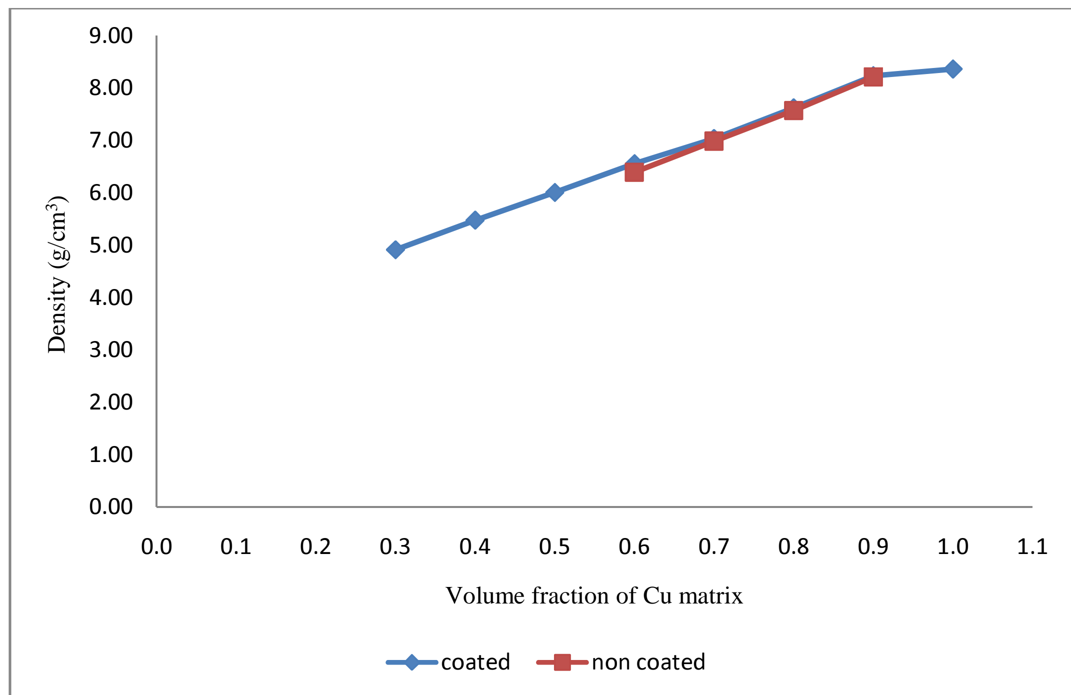

Figure 4.10: Density measured using pycnometer for both Cu-coated SiC and non-coated SiC reinforcement in CuSiC composites.

For Cu-coated SiC reinforcement in the composites, the result obtained from all measured, bulk or pycnometer showed slightly higher density compared to non-coated SiC reinforcement. This might due to the better interface bonding between Cu matrix and Cu-coated SiC in the composites as discussed previously in section 4.3.

The fraction of the total void volume or the porosity can be determined by the equation (Shu 2003):

$$P_f = 1 - \frac{\rho}{\rho_o}$$

where P_f is the pore volume fraction, ρ is the measured density and ρ_o is the theoretical density. Besides, the porosity also can be determined by the difference of bulk density measured using density meter and the true density from pycnometer measurement.

Figure 4.11 showed the porosity percentage of the specimens. As the density trend increases, the porosity percentage is expected to behave oppositely. This might be due to the entrapped H_2 gas during the electroless coating process.

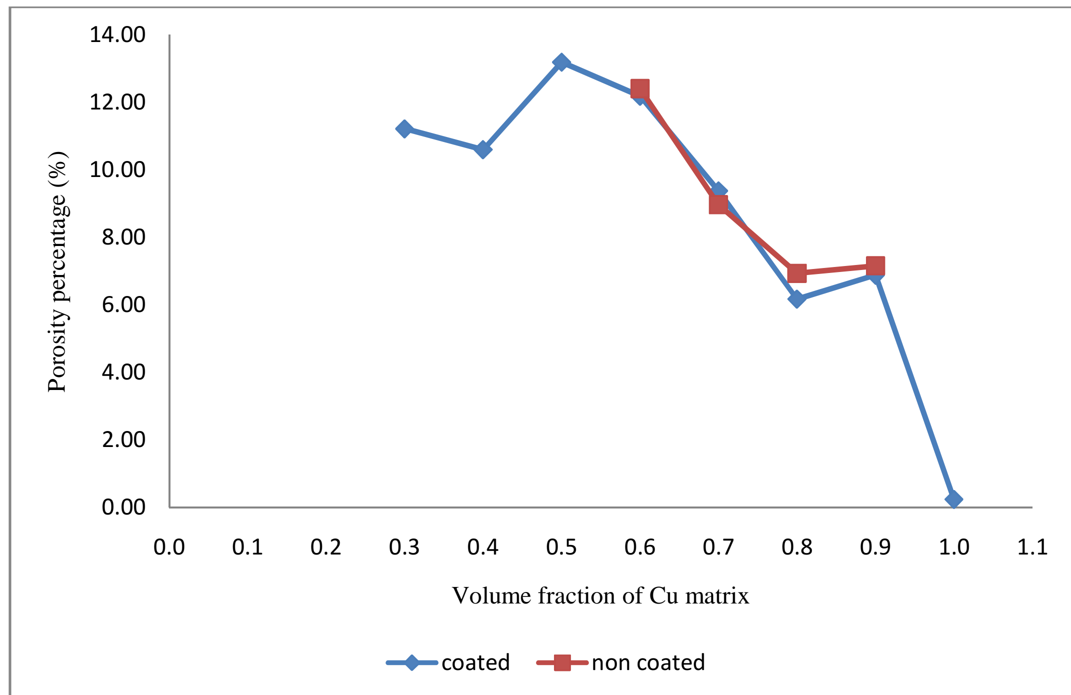

Figure 4.11: Percentage of porosity for both Cu-coated SiC and non-coated SiC reinforcement in CuSiC composites.

CHAPTER 5

CONCLUSION AND RECOMMENDATION

5.1 Conclusion

Nowadays, aluminum matrix reinforced with silicon carbide particle (Al-SiC) is widely used as the thermal management materials for electronics packaging. However, it has limitation on the coefficient thermal expansion (CTE) properties since it only can be altered between 6.2 to 23 ppm/K as well as the thermal conductivity which limited to 220 W/m.K. Therefore, the invention of copper matrix reinforced with silicon carbide particles (Cu-SiC) is expected to improve on the thermal properties since copper has almost double the thermal conductivity compared to aluminum.

CuSiC composites have the interface problem between the copper matrix and the silicon carbide particles reinforcement due to no bonding between the two constituents. In order to improve the bonding issue, the reinforcement is coated with a thin copper film by using electroless coating technique to obtain homogeneous copper deposits on SiC particles. Then, the Cu-SiC composite was fabricated by different volume fraction of the SiC reinforcement to analyse the behavior of the properties. The composites is compared between Cu-coated SiC particles reinforcement and non-coated SiC particles reinforcement.

From the XRD pattern of a sample of CuSiC composite, the peaks that exist is similar to the raw materials' XRD peaks which are spheroidal Cu powder and SiC particles. Before performing the electroless coating, the surface of SiC particles need to be cleaned from unwanted contaminants through ultrasonic cleaning in a solvent. Then,

the surface is sensitized and activated to seed the surface for Cu deposits. Then, the electroless coating technique is conducted in a electroless copper coating bath under suitable temperature and pH of the coating solution. Then, the Cu-coated SiC particles need to be dryed at 600°C for 2 hours. From SEM images on the raw SiC particles, the unwanted contanminants can be seen. After ultrasonic cleaning in solvent, no contaminant observed under SEM image. After activation process, SEM images have shown the surface of SiC that already seeded with catalytic element for Cu deposits. After coating process, the SEM image shows the Cu deposits on the SiC particles.

Particle size distribution is another characteristic which conducted in this research work. The particles size distribution was performed on the raw SiC particles, after ultrasonic cleaned SiC particles, after sensitizing and activation of the SiC particles as well as after Cu-coating on SiC particles. The size distribution showed that, after cleaned the SiC, no other contaminant less than 10 microns left in the powder. Then, after sensitizing and activation, the mean distribution is slightly higher due to catalytic elements which attached to the SiC particles. Then, after Cu-coating process, the mean particle size distribution gow higher because of the Cu deposits on SiC particles.

Fabrication of the CuSiC composites is performed using powder metallurgy methodology. The Cu matrix and SiC reinforcement (both Cu-coated and non-coated) is mixed via ball milling method and pressed in a customized mold with 50kN uniaxial compaction load. Then, the compacted samples are sintered at 925°C for 2 hours in argon atmosphere. After that, the samples were measured for density using analytical balance, vernier caliper, density meter and also pycnometer. The density trend shows that, as the volume fraction of SiC reinforcement increased, the density decreased. For Cu-coated SiC reinforcement, the density is slightly higher compare to the non-coated

SiC reinforcement. For the percentage of porosity, the trend shows oppositely of the density trend. This is because, the higher the density, the lower the porosity.

5.2 Recommendation

Due to the time constrain, this research work still have a lot of areas to be explored. The study on the thermal conductivity, CTE, and also the mechanical properties of the CuSiC composites are recommended in future. With these further studies and characterizations, the improved development of CuSiC via electroless coating process can be achieved.

BIBLIOGRAPHY

Peter Krieg, The Red Brick Wall, Pile Systems 2004.

Carl Zweben, *Thermal Materials Solve Power Electronics Challenges, Power Electronics Technology*, February 2006.

M.A. Occhionero, R.W. Adams, K.P. Fennessy, R.A. Hay, *"Aluminum Silicon Carbide (AlSiC) for Thermal Management Solutions and Functional Packaging Designs"* proceedings of the Annual IMAPS Conference, San Diego CA, October, 1998.

N. Koura, *Electroless Plating of Silver, Electroless Plating: Fundamentals and Applications*, American Electroplaters and Surface Finishers Society, Chapter 17, Page 441, 1990.